applied sciences

MDPI

Article

Surface Optimization of Micro-Integrated Reflective Optical Elements by Thermoset Injection Molding

Thomas Guenther [1,2,*], Lars Diegel [2], Marcel Roeder [2], Marc Drexler [2], Mehmet Haybat [2], Peter Wappler [2], Mahdi Soltani [1,2] and André Zimmermann [1,2]

1 Institute for Micro Integration (IFM), University of Stuttgart, Allmandring 9B, 70569 Stuttgart, Germany; Mahdi.soltani@ifm.uni-stuttgart.de (M.S.); Andre.zimmermann@ifm.uni-stuttgart.de (A.Z.)

2 Hahn-Schickard e.V., Allmandring 9B, 70569 Stuttgart, Germany; Lars.diegel@hahn-schickard.de (L.D.); Marcel.roeder@hahn-schickard.de (M.R.); Marc.drexler@hahn-schickard.de (M.D.); Mehmet.haybat@hahn-schickard.de (M.H.); Peter.wappler@hahn-schickard.de (P.W.)

* Correspondence: Thomas.guenther@ifm.uni-stuttgart.de; Tel.: +49-711-68583713

Received: 20 May 2020; Accepted: 12 June 2020; Published: 18 June 2020

Abstract: Thermoset materials offer a multitude of advantageous properties in terms of shrinkage and warpage as well as mechanical, thermal and chemical stability compared to thermoplastic materials. Thanks to these properties, thermosets are commonly used to encapsulate electronic components on a 2nd-level packaging prior to assembly by reflow soldering on printed circuits boards or other substrates. Based on the characteristics of thermosets to develop a distinct skin effect due to segregation during the molding process, the surface properties of injection molded thermoset components resemble optical characteristics. Within this study, molding parameters for thermoset components are analyzed in order to optimize the surface quality of injection molded thermoset components. Perspectively, in combination with a reflective coating by e.g., physical vapor deposition, such elements with micro-integrated reflective optical features can be used as optoelectronic components, which can be processed at medium-ranged temperatures up to 230 °C. The obtained results indicate the general feasibility since Ra values of 60 nm and below can be achieved. The main influencing parameters on surface quality were identified as the composition of filler materials and tool temperature.

Keywords: thermoset; injection molding; micro-optics; reflective optics; surface characterization

1. Introduction

Micro-optical systems are essential in everyday life and industrial applications. This includes applications such as mobile phone cameras, driving assistance systems, light barriers, endoscopes, optical data storage, motion controllers, inspection systems, illumination units and many more [1–6]. Optical components are omnipresent, however very unobtrusive due to rapid advances in miniaturization and micro integration, making them non-observable for the user in most cases. However, behind these applications is a very versatile market for optical technologies, which is currently developing at an impressive speed of 6–8% p.a. [1,7]. Additionally, being a key-enabling technology for the European Union, the funding for developments of innovative, highly integrated optics is a priority [1,8].

Current developments are more and more based on polymer technologies as the performance of these materials is improving continuously. Tailoring the properties of the materials by the suppliers opens new doors and offers the possibility to unlock untapped potentials for a multitude of innovative applications [9]. At the same time, costs can be reduced compared to glass components due to the

methods of mass production for polymers such as injection molding [10–13]. Furthermore, more degrees of freedom in terms of three-dimensional processing are possible.

Many applications already employ injection molding of optical components. In particular, injection molded lenses, microlenses and micro-structured lenslets or arrays made of thermoplastic materials dominate the market due to their wide range of applicability and the availability of well know material [14–22]. Newer applications with more challenging requirements employ silicones, which require more sophisticated molding processes and have strong limitations in complex hybrid assemblies [22]. Injection molding of thermoset materials is comparable to silicone processing in terms of tool requirements and process flow. However, thermosets offer the advantage of being provided as granulate making storage and molding significantly easier in comparison to silicones, and they are the established standard in electronic packaging and higher-level assemblies for the last decades.

Thermoset materials are not very common in the field of optics since non-filled materials with the required transparency have very high shrinkage rates, large coefficients of thermal expansions and the tendency of yellowing at UV light exposure. However, the surfaces of standard package electronic components using thermosets with tailored filler materials are mirror-like. Smallest defects in the mold tool or deviations of the designed mold flow appear as unacceptable defects in the view of a customer, even though these defects do not present any functional limitations and are, in most cases, less severe as non-visible scratches from demolding or joint lines in thermoplastic components. The ability to form such surfaces during the molding process leads to the idea of using thermosets as reflective optical elements, or moreover of integrating micro-optical features in thermoset components, either as stand-alone components or as additional features in electronic packaging.

The injection molding process of thermoset materials can be outlined as follows: the molding tool is closed and the injection process starts. The melt is pressed through an opened nozzle into the gate system. A laminar flow with $Re \leq 2300$ is to be derived to avoid turbulences without voids being trapped in the melt [23]. The process differs at two distinct characteristics from processing of thermoplastics. The higher difference in temperature of the melt to the tool in thermoplastic injection molding leads to a surface zone, causing solidification effects of the melt at the wall between melt and tool. Thermosets in contrast, have no significant temperature difference between melt and tool preventing the solidification effect. The second characteristic is the flow rate of the melt front. Thermosets contain significantly more additives, not only consisting of filler materials such as fibers or spheres, which are deployed to optimize flow properties. Amongst those are, beside fillers, resin and hardener, flame suppressants, anti-adhesives for improved ejection as well as adhesives for improved adhesion to inserts to be encapsulated, ion binders, dyes, low-stress additives for reduced internal stresses, and catalysts for accelerated polymerization [24,25]. These additives lead to a higher sliding rate between the wall of the tool and the melt, causing a more linear profile of the flow front as in the case of thermoplastics. Due to the changed flow profile and the larger size of the fillers, the fillers cannot segregate at the wall, leading to a low viscosity lubricating film at the interface [26]. The skin layer consists mostly of pure epoxy resin, which typically has very low roughness values. Fillers and additives are located within the bulk material (Figure 1) [27,28].

Parameters, which are assumed to influence the surface quality, are the choice of filler material, the direction of injection in regard to the functional area, injection velocity, tool temperature and injection pressure as well as holding pressure.

Fibers are commonly used filler materials in both thermoplastics and thermoset materials. The main advantage of the fibers is the availability of different materials, the achievable mechanical strength and the developing coefficient of thermal expansion (CTE) in regard to matching the components with printed circuit board (PCB) technology and, hence, to reduce induced stresses in the solder joints. However, anisotropic effects and possible needle sticking into the skin layer may occur. Glass spheres in return have better properties in terms of isotropy, but show adverse effects regarding shrinkage and CTE-mismatch.

The direction of injection plays a vital role as the melt front resembles a non-pressurized volume, which pushes ahead inhomogeneous large amounts of fillers and experiences other temperature gradients due to compressed air, which needs to be pushed out of the mold cavity. Constituent parts such as water, styrene or formaldehyde show phase transformations. Volume expansion in combination with the large ratio of filler material causes porosity. Thus, the plug must not come to rest in the functional area, neither must the plug hit an optical surface of the mold tool in a perpendicular angle causing potential damages of the surface.

Comparing thermoset molding with thermoplastic molding, direct process parameters need to be considered. The particularly reduced pressure of 50–250 bar in thermoset molding compared to 800–1200 bar in thermoplastic molding leads to the fact, that deviations from ideal set points are more sensitive due to their total percentage in thermoset molding, making process control more challenging. The aim of this study is to study these effects and their influence on resulting surface properties.

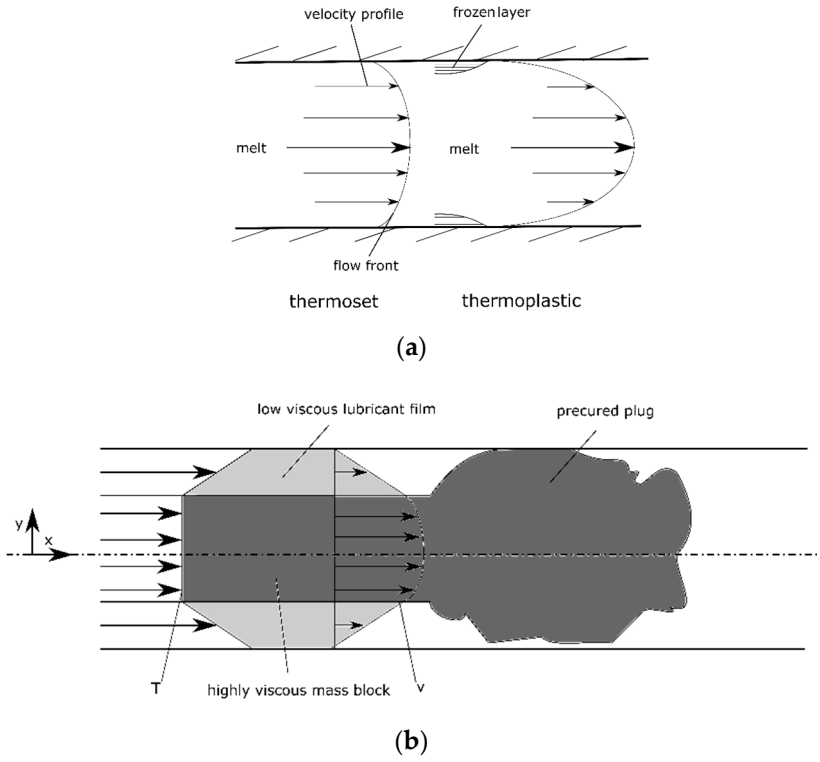

Figure 1. (**a**) Comparison of flow profiles of thermoset and thermoplastic injection molding. (**b**)Detail of flow profile of thermoset injection molding according to the model of block-shear flow. Highly viscous melt remains at the flow front and within the core while a low viscous sliding zone without fillers is formed at the surface. The surface texture is reproduced very detailed by the low viscous resin. Within the mass block, fillers and additives are contained. The undefined precured plug needs to be removed prior to entering the mold.

2. Materials and Methods

2.1. Materials

On the course of studying the surface optimization of thermoset injection molding for micro-integrated reflective optical elements, mold inserts for a universal molding tool with optical properties were designed and manufactured. X135CrMoV12 tooling steel was chosen because of its high resistance to abrasion, its low CTE as well as its high Young's modulus. Furthermore, preliminary studies have shown a low adhesion of thermosets to this steel due to its high chromium content. However, since steel is not suitable for machining optical surfaces as mill bits made of diamond required for optical surfaces get blunt on ferritic materials due carbon diffusion [29], the nozzle sided

inserts were hardened and coated with NiP (SuNiCoat, CZL Tilburg BV Surface Technology, Tilburg, The Netherlands). The NiP coating was machined using a 3 mm diameter diamond radius cutter (Horn GmbH, Tübingen, Germany).

The epoxy molding compounds chosen were types filled with glass spheres and glass fibers. Both compounds are available as granulate for injection molding. Their dimensional stability, and thus the replication constancy, is stated by the manufacturer to be "very good".

2.2. Mold Design

The mold design was based on platelet design, but inherited two major features: an optical surface with a 15° angle was implemented on one side (Figure 2b), while the other side-accommodated features for dimensional measurements (Figure 2a). The 15° angle was chosen to have both, a possible tilted mirror area and an angle that is still small enough to remain within the acceptance angle of white light interferometric measurement (typically max. 30°).

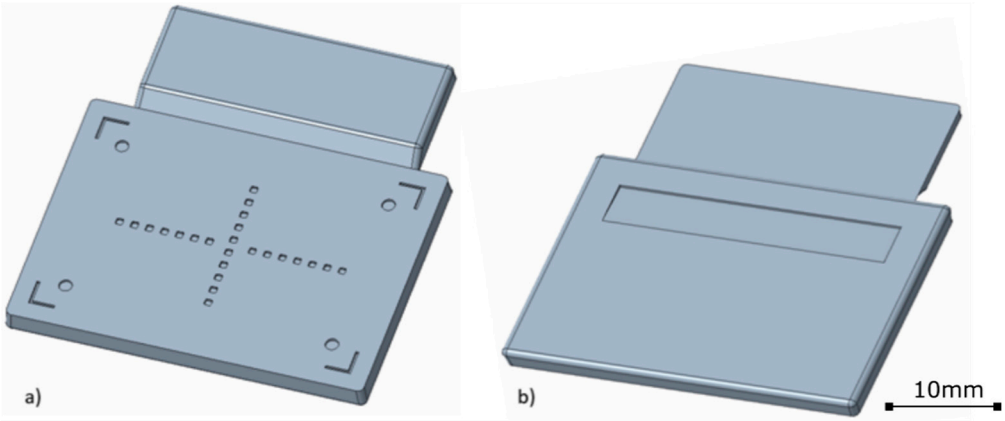

Figure 2. (**a**) one side of the platelet design was used to implement measurement features for shrinkage and warpage. (**b**) on the other side a tilted area for surface optimization was implemented.

The determination of the influence of the direction of injection requires a mold tool design, which allows for injection orthogonal and longitudinal to the mirror surface. A selective point of injection was designed, which has been realized by a sliding feed. The general sprue had an intercepting structure for catching the plug which formed between nozzle and gate. Subsequent plug formation was addressed by an overflow structure in the cavity, causing the melt front to be positioned outside of the functional part (Figure 3).

The molding tool was machined using a 3-axis milling center (CMX 600V, DMG-Mori AG, Bielefeld, Germany). The measurement side of the cavity was further processed by precision milling employing a 3-axis high-speed cutting center (PFM 24cc, Primacon GmbH, Peissenberg, Germany). The mirror side of the cavity was machined into the NiP coated insert using a 5-axis ultraprecison machining (Micromaster5x, Kugler GmbH, Salem, Germany). A diamond cutter with a 3 mm radius was chosen to ensure a smooth surface of the mirror surface. Standard features were cut using CBN thoric mill bits. The edges were radiused and the wall was tapered to ensure problem-free ejection (Figure 4)

2.3. Injection Molding

The injection molding was performed using a molding machine with vertical arrangement and a thermoset molding unit (375V, Arburg). A full factorial design of experiment (DoE) with five factors and two levels each was defined employing factorial design software (Minitab V19, Minitab Inc, State College, PA, USA). Thus, 32 design points with 8 samples each lead to a set of 256 components to be investigated. The parameters for the design of experiment and their corresponding levels are shown in Table 1. The DoE was adapted regarding the sequence to ensure a reasonable workflow for injection

molding. The varying factor of tool temperature and direction of injection molding was changed to minimize machine set-up time.

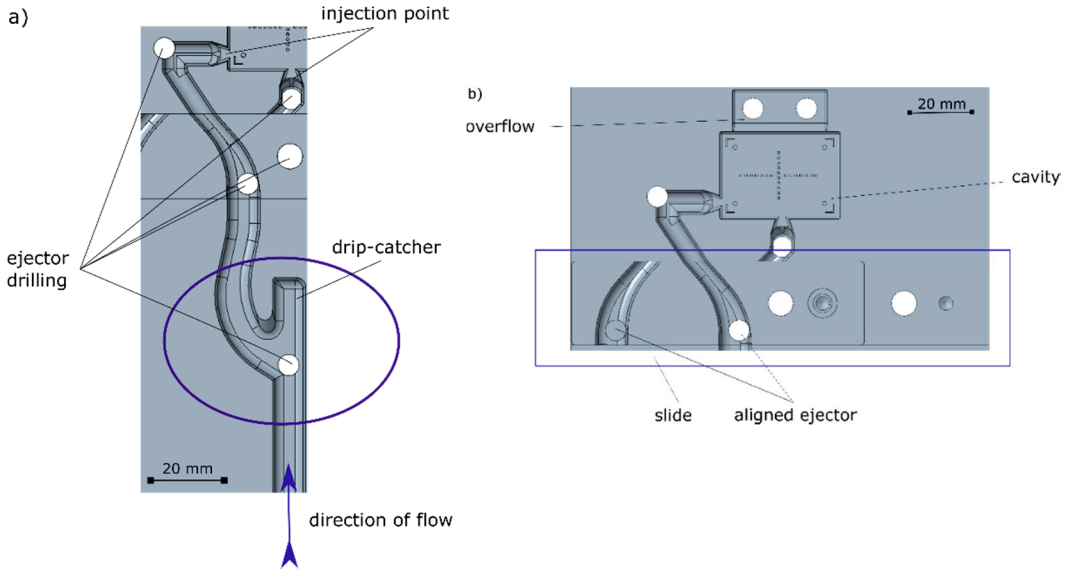

Figure 3. (**a**) sprue with plug interceptor. (**b**) sliding feed for selection of the direction of injection with point of injection from the left (longitudinal to the mirror surface) and from the center (orthogonal to the mirror surface).

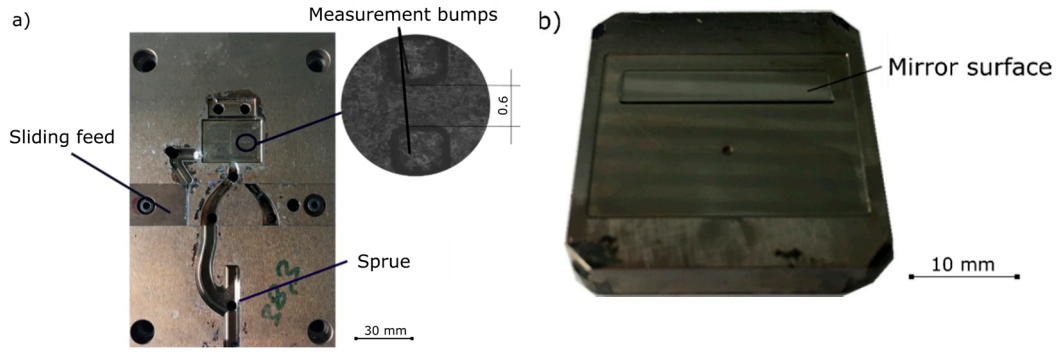

Figure 4. (**a**) measurement side of the cavity. Bumps for dimensional analysis were milled using precision machining. (**b**) mirror side of the cavity. The reflective surface was milled in NiP coating using ultra-precision machining employing diamond mill bits.

Table 1. Parameters for the design of experiment.

DoE nr.	Material	Factor	Corresponding Levels	
1	Glass sphere filled	Holding pressure [bar]	300	700
		Direction of injection	Longitudinal	Orthogonal
		Holding time [s]	40	70
		Tool temperature [°C]	180	200
2	Fiber filled	Holding pressure [bar]	330	770
		Direction of injection	Longitudinal	Orthogonal
		Holding time [s]	5	20
		Tool temperature [°C]	150	190

3. Results

Three output variables were recorded: surface roughness Ra [nm], warpage [µm] and shrinkage [%]. The applying design points refer to the standard order given by the DoE, which is shown in Appendix A, Table A1. Design point 11 could not be molded due to incomplete curing and, thus, impossible ejection of the parts.

3.1. Measurements

The surface roughness Ra was measured on the reflective section of the component using white light interferometry (WLI). A 50× objective was used, leading to a field of view with 0.75 mm width (Figure 5). Ra Values between 55 and 100 nm were achieved with the glass sphere filled material. The glass fibers filled material showed values which are a factor of approximately 2.5× higher.

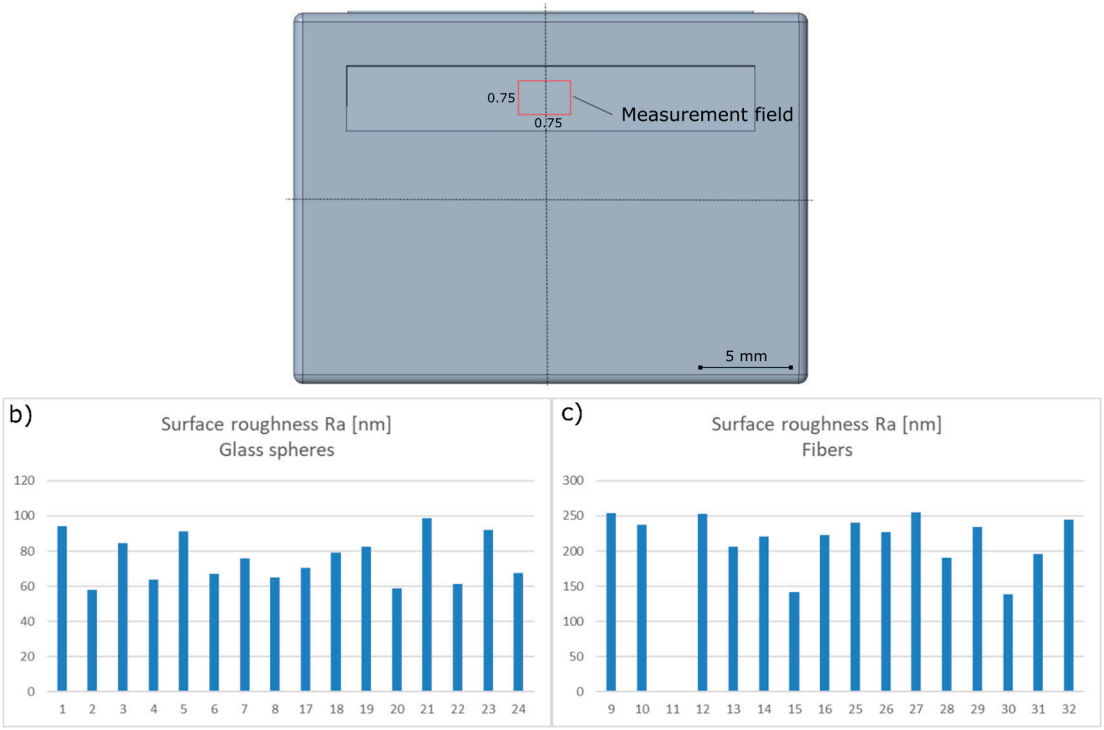

Figure 5. (**a**) measurement field for surface roughness Ra using WLI. (**b**) Ra values of glass sphere filled material with a standard deviation of 13.1 nm. (**c**) Ra values of fiber filled material with a standard deviation of 36.0 nm.

The warpage was measured using WLI. Technically, warpage related to a momentum across any translatory axis (X,Y,Z). If several momentums apply at the same time, aspheric surfaces may develop, which are difficult to capture. The integrated features were used to determine these values, consisting of several squared trenches with 0.1 mm width. The 24 squares were arranged in a cross constellation with a spacing of 0.6 mm between each square. Since the trenches present a recess structure with an easily detectable edge, the x and y positions were measurable without any further data processing. To determine the z position, a point of origin was determined in the center of the cross. Each square was measured in z and the difference to the point of origin was recorded. The measurement values were averaged to allow for a comparable value for this study (Figure 6).

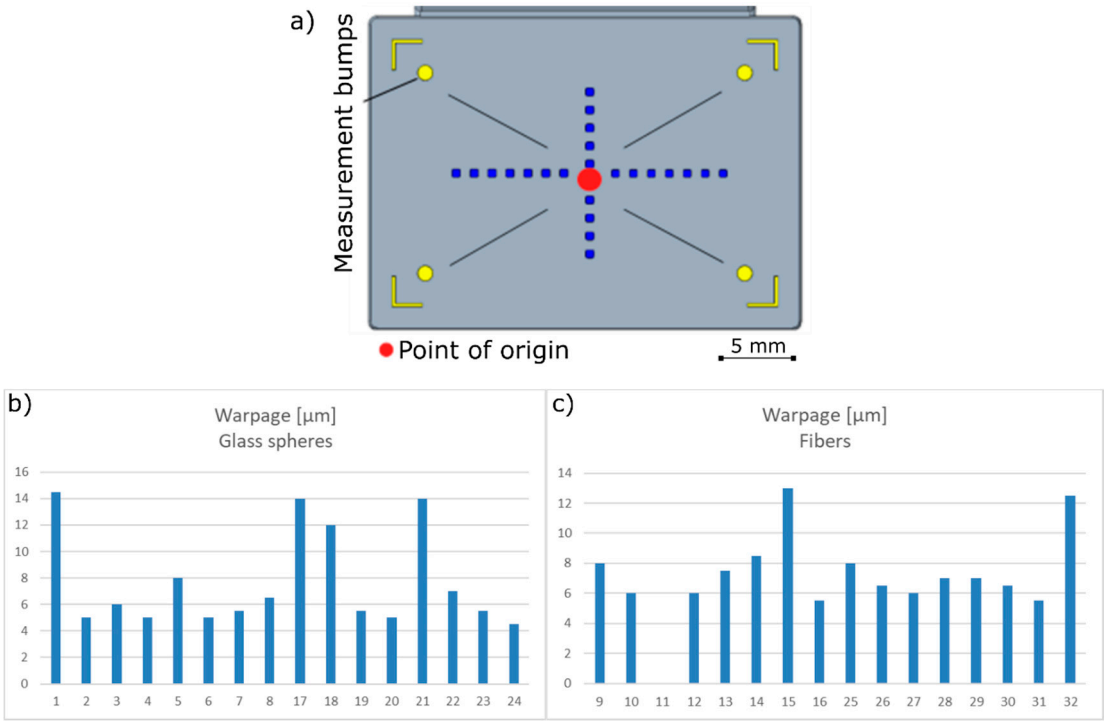

Figure 6. (**a**) measurement field for warpage detection. (**b**) Measured values of the warpage of glass sphere filled material with a standard deviation of 3.56 µm. (**c**) Measured values of the warpage of fiber filled material with a standard deviation of 2.22 µm.

Shrinkage was determined by measuring the length and width of the samples. The difference to the dimensions of the cavity was determined. The averaged values are displayed in Figure 7.

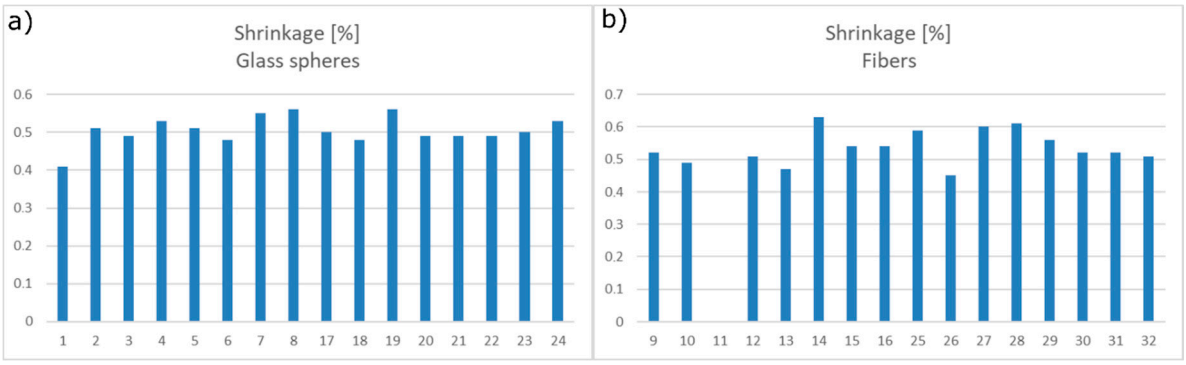

Figure 7. Shrinkage measurement of length and width in comparison to the original dimensions. (**a**) Measurements of shrinkage of glass sphere filled material with a standard deviation of 0.036%. (**b**) Measurements of shrinkage of fiber filled material with a standard deviation of 0.05%.

3.2. Evaluation

Before starting with the interpretation of the results, a plausibility check has to be conducted, e.g., using Minitab, in order to detect any outliers, transposed digits or typos. No irregularities are to be mentioned. As mentioned before, Minitab is the statistics software used in this work for analyzing the results. In this kind of studies, it is common to make use of Pareto diagrams of standardized effects as well as of main effect diagrams in order to identify and evaluate the significance of the impact factors and their interactions on the response. While the fiber-filled material showed no significant effects within the chosen factor range and thus has not been investigated further, the glass spheres filled material revealed a strong relation between surface quality and tool temperature. Higher tool

temperatures lead to smoother surfaces (Figure 8; higher slopes in the main effect diagram). However, variations of the direction of injection, holding time and pressure did not lead to any significant improvements. Warpage was mostly influenced by the direction of injection. Particularly, injection orthogonally to the reflective area leads to a geometrically balanced mold flow situation. No adverse effects on surface quality could be observed. Furthermore, an increased tool temperature improved warpage effects significantly by more than 50% (Figure 9). Evaluation for shrinkage showed barely a significant impact on the direction of injection. Other correlations for shrinkage could not be detected.

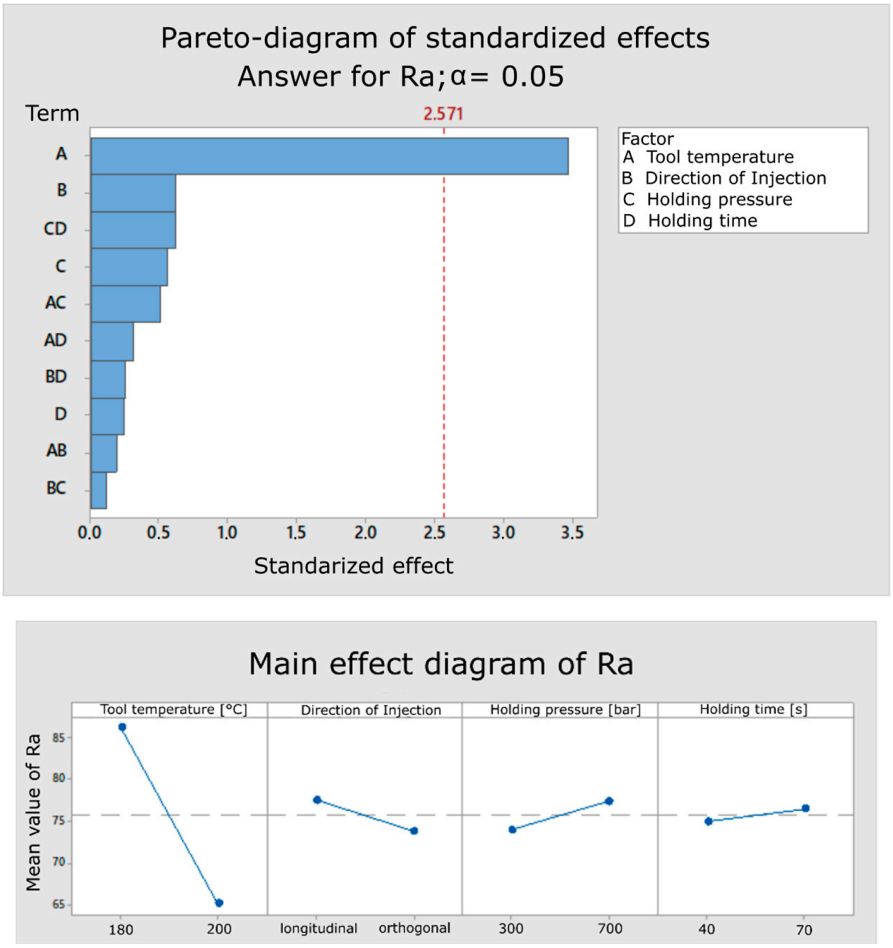

Figure 8. Evaluation of surface roughness of spherical glass-filled thermoset. (**Top**) Pareto diagram with the threshold for significance. (**Bottom**) main effect analysis.

As seen in prior works [30], regarding filled thermoplastics, the geometry of the fillers as well as their aspect-ratio play a pivotal role in defining the filler orientation and, hence, the isotropy of the material and even in creating a filler-free molding skin at the surface. Fibers are subjected to rotational forces caused by flow velocities and, thus, more susceptible to reach the surface and affect its quality. Similar effects could emerge during thermoset injection molding, too.

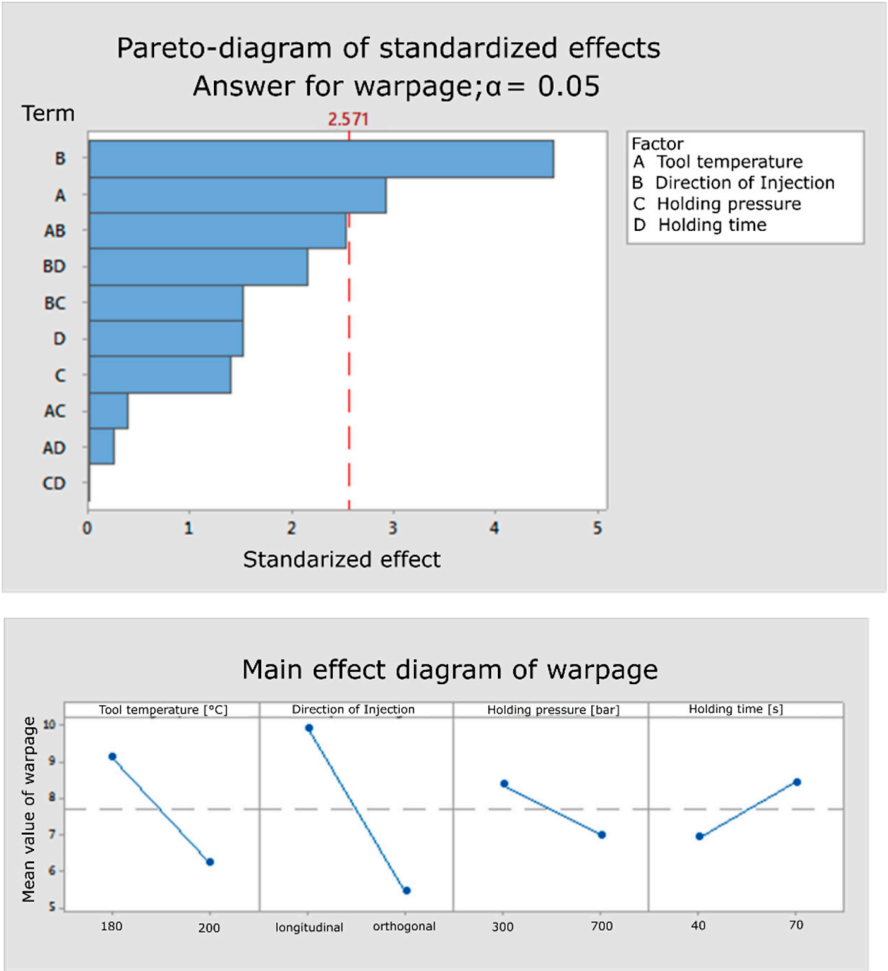

Figure 9. Evaluation of warpage of spherical glass-filled thermoset. (**Top**) Pareto diagram with the threshold for significance. (**Bottom**) main effect analysis.

4. Discussion

The optimization of the surface quality towards reflective optical elements made by thermoset injection molding showed promising results. Surface quality with values close to 50 nm were possible. Technical optics with the purpose of signal reflection may be possible, in particular in combination with subsequent sputter processes such as Cr/Au, Ag or other reflective coatings. While the achieved values may appear low, the conducted measurements provide only a first insight into the potential of using thermosets as optical elements.

Conducting the measurements presented a challenge for itself. On one side, the high reflectivity caused strong difficulties applying optical measurement tools due to highly reduced angles of acceptance, on the other side tactile measurements may destroy the polymeric surfaces during measurement, thus presenting no valid method. Furthermore, the surfaces created using a radius mill bit are prone to effects such as waviness. More dedicated analysis methods are required, which allow filtering of those effects from the measurement of the surface roughness. Fast fourier transformations on surface area roughness (Sa) measurements according to ISO25178 need to be applied. Also, fly cutting the optical inserts may be implemented into the tool cavity to avoid milling patterns in future investigations. However, with the requirement of absolute tolerances of features within a mold cavity, this option would increase the tolerances significantly.

The dimensional analysis showed shrinkage values in the range of 0.5% dependent on the parameter set chosen. On the course to achieve optical elements, injection molding with a precision of ±2 µm and better is desired. Iterations in tool making can be applied to achieve the best absolute

values. Consequently, further analysis should focus on the variations of shrinkage dependent on environmental parameters and varying material batches. Nonetheless, the best warpage result with an absolute tolerance of down to +4.5 µm could be achieved with the best parameter set.

A preceding application development employing the technique for functional components may provide insights into the anticipated functionality: within this development, micromirrors were machined by ultra precision milling resulting in a mold roughness Ra 25 nm. An orthogonal direction of injection was chosen, leading to a molded component with a surface roughness of Ra with 66.9 nm with a standard deviation of 29.2 nm. The thermoset components were sputter-coated with 60 nm chromium and 300 nm gold after molding and the transmission loss was measured. An average transmission loss of 1.25 dB could be achieved. The high standard deviations could be attributed to highly differing values in the center of the mirror structure compared to the outer areas. With the improved processing parameters in addition to extended measures of mold flow control such as drip catchers and overflow structures, further improvements on homogeneity and quality of surface properties and, thus, on transmission can be expected, lowering the transmission loss towards 0.6 dB. However, further studies towards surface replication by thermoset molding with the focus on inhomogeneities are required.

5. Conclusions

The study presents a first test using thermoset materials as polymeric optical elements. An application centered approach was chosen to identify the impact factors on the surface quality and dimensional reproduction using thermoset injection molding. The results showed the potential of thermoset materials as reflective optical elements. Insights into the applicability were gained and the main impact factors influencing the process could be identified.

The combination of improved surface roughness while allowing to achieve outstanding dimensional accuracy of <±10 µm tolerance renders the material as an ideal option for micromolding of small parts as well as highly accurate parts. Besides optical analysis, the mechanical analysis may show that this technique can replace also other functional thermoplastic parts, which require higher thermal, mechanical and chemical resistance.

However, relating to the aim of optical application, further determining factors became obvious. In respect to material choice, glass sphere filled materials are more promising than glass fiber-filled materials. Respectively, further materials need to be tested, whereas material compositions can be varied towards optimization of surface properties. Tool temperature was identified as the most influencing parameter. Since the initial study started as full factorial DoEs, this particular factor allows for a more selective analysis with a more finely graded and further ranging parameter sweep. To better understand the surface properties, it is required to study the bulk material in more detail.

Author Contributions: T.G. conceptualized the study, wrote the manuscript and supervised the project. L.D. conceptualized the DoE and conducted the experiments. M.R. provided the technical requirements and tool selection. M.D. was in charge of tool manufacturing. M.H. supervised and operated the injection molding process. P.W. conducted experiments on material selection. M.S. was responsible for data analysis and critically revised the manuscript. A.Z. critically revised the manuscript, provided facilities to conduct the research and provided the funding. All authors have read and agreed to the published version of the manuscript.

Funding: This research was financed by budgetary funds of the University of Stuttgart and Hahn-Schickard e.V.

Acknowledgments: The authors want to thank Hurasky-Schönwerth from Andreas-Stihl AG & Co.KG for his advice on the DoE conceptualization.

Conflicts of Interest: The authors declare no conflict of interest.

Appendix A

Table A1. Combined experimental data set.

Standard Order	Processing Order	Tool Temp-Erature [°C]	Direction of Injection	Holding Pressure [°C]	Filler Geometry	Holding Time [s]	Roughness Ra [nm]	Shrinkage [%]	Warpage [µm]
1	1	180	longitudinal	300	Spheres	40	94.306	0.41	14.5
2	15	200	longitudinal	300	Spheres	40	57.77	0.51	5
3	7	180	orthogonal	300	Spheres	40	84.49	0.49	6
4	12	200	orthogonal	300	Spheres	40	63.64	0.53	5
5	4	180	longitudinal	300	Spheres	40	91.055	0.51	8
6	14	200	longitudinal	700	Spheres	40	67.03	0.48	5
7	8	180	orthogonal	700	Spheres	40	75.66	0.55	5.5
8	9	200	orthogonal	700	Spheres	40	65.045	0.56	6.5
9	32	150	longitudinal	300	Fibers	5	254	0.52	8
10	19	190	longitudinal	300	Fibers	5	237.15	0.49	6
11	28	150	orthogonal	300	Fibers	5	not	processable	
12	21	190	orthogonal	300	Fibers	5	253.06	0.51	6
13	30	150	longitudinal	700	Fibers	5	206.415	0.47	7.5
14	17	190	longitudinal	700	Fibers	5	220.695	0.63	8.5
15	27	150	orthogonal	700	Fibers	5	141.27	0.54	13
16	22	190	orthogonal	700	Fibers	5	222.405	0.54	5.5
17	3	180	longitudinal	300	Spheres	70	70.385	0.5	14
18	16	200	longitudinal	300	Spheres	70	79.27	0.48	12
19	5	180	orthogonal	300	Spheres	70	82.625	0.56	5.5
20	10	200	orthogonal	300	Spheres	70	58.935	0.49	5
21	2	180	longitudinal	700	Spheres	70	98.92	0.49	14
22	13	200	longitudinal	700	Spheres	70	61.41	0.49	7
23	6	180	orthogonal	700	Spheres	70	92.035	0.5	5.5
24	11	200	orthogonal	700	Spheres	70	67.565	0.53	4.5
25	31	150	longitudinal	300	Fibers	20	241.035	0.59	8
26	18	190	longitudinal	300	Fibers	20	226.9	0.45	6.5
27	25	150	orthogonal	300	Fibers	20	254.78	0.6	6
28	24	190	orthogonal	300	Fibers	20	190.54	0.61	7
29	29	150	longitudinal	700	Fibers	20	233.94	0.56	7
30	20	190	longitudinal	700	Fibers	20	138.775	0.52	6.5
31	26	150	orthogonal	700	Fibers	20	195.505	0.52	5.5
32	23	190	orthogonal	700	Fibers	20	245.025	0.51	12.5

References

1. Photonics 21. *Photonics—A critical Key Eneabling Technology for Europe: Role and Impact of Photonics in H2020*; VDI Technologiezentrum GmbH: Dusseldorf, Germany, 2018.
2. Yun, Z.; Lam, Y.L.; Zhou, Y.; Yuan, X.; Zhao, L.; Liu, J. Eyepiece design with refractive-diffractive hybrid elements. In *Current Developments in Lens Design and Optical Systems Engineering, the Proceedings of the International Society for Optics and Photonics, International Symposium on Optical Science and Technology, San Diego, CA, United States, 24 October 2000*; Society of Photo Optical: Bellingham, WA, USA, 2000; Volume 4093, pp. 474–481.
3. Cox, J.A.; Fritz, T.A.; Werner, T.R. Application and demonstration of diffractive optics for head-mounted displays. In *Helmet- and Head-Mounted Displays and Symbology Design Requirements, the Proceedings of the International Society for Optics and Photonics, SPIE's International Symposium on Optical Engineering and Photonics in Aerospace Sensing, Orlando, FL, USA, 10 June 1994*; Society of Photo Optical: Bellingham, WA, USA, 1994; Volume 2218, pp. 32–41.
4. Kress, B.; Starner, T. A review of head-mounted displays (HMD) technologies and applications for consumer electronics. In *Photonic Applications for Aerospace, Commercial, and Harsh Environments IV, the Proceedings of the International Society for Optics and Photonics, SPIE Defense, Security, and Sensing, Baltimore, MD, USA, 29 April–1 May 2013, Society of Photo Optical: Bellingham, WA, USA, 2013*; Volume 8720, p. 87200A.
5. Nakai, T.; Ogawa, H. Research on multi-layer diffractive optical elements and their application to camera lenses. In *Diffractive Optics and Micro-Optics*; OSA Trends in Optics and Photonics Series; paper DMA2; Magnusson, R., Ed.; Optical Society of America: Washington, DC, USA, 2002; Volume 75.
6. Early, J.T.; Hyde, R.; Baron, R.L. Twenty-meter space telescope based on diffractive Fresnel lens. In *UV/Optical/IR Space Telescopes: Innovative Technologies and Concepts, the Proceedings of the International Society for Optics and Photonics, Optical Science and technology, SPIE's 48th Annual Meeting 30 January 2003, San Diego, CA, USA*; Society of Photo Optical: Bellingham, WA, USA, 2004; Volume 5166, pp. 148–157.
7. Spectaris—German Industry Association for Optics, Photonics, Analytical and Medical Technology. *Spectaris, Trend Report Photonik 2019/2020—Markets, Developments, Potentials*; Federal Ministry for Education and Research Germany: Berlin, Germany, 2019.
8. Committee Optical Technologies. *Agenda Photonik 2020*; Federal Ministry for Education and Research Germany: Berlin, Germany, 2016.
9. Brinksmeier, E.; Riemer, O.; Gläbe, R. *Fabrication of Complex Optical Components*; Springer-Verlag: Berlin/Heidelberg, Germany, 2013.
10. Lin, C.-M.; Hsieh, H.-K. Processing optimization of fresnel lenses manufacturing in the injection molding considering birefringence effect. *Microsyst. Technol.* **2017**, *23*, 5689–5695. [CrossRef]
11. Brinksmeier, E.; Gläbe, R.; Schönemann, L. Review on diamond-machining processes for the generation of functional surface structures. *CIRP J. Manuf. Sci. Technol.* **2012**, *5*, 1–7. [CrossRef]
12. Roeder, M.; Schilling, P.; Hera, D.; Guenther, T.; Zimmermann, A. Influences on the fabrication of diffractive optical elements by injection compression molding. *J. Manuf. Mater. Process.* **2018**, *2*, 5. [CrossRef]
13. Lee, B.-K.; Kim, D.S.; Kwon, T.H. Replication of microlens arrays by injection molding. *Microsyst. Technol.* **2004**, *10*, 531–535. [CrossRef]
14. Beich, W.S. Injection molded polymer optics in the 21st-Centtury. In Proceedings of the SPIE Conference on Optics and Photonics 5865J, San Diego, CA, USA, 22 August 2005.
15. Kim, D.S.; Lee, H.S.; Lee, B.-K.; Yang, S.S.; Kwon, T.H.; Lee, S.S. Replications and analysis of microlens array fabricated by a modified LIGA process. *Polym. Eng. Sci.* **2006**, *46*, 416–425. [CrossRef]
16. Levoy, M.; Hanrahan, P. Light field rendering. In Proceedings of the 23rd Annual Conference on Computer Graphics and Interactive Techniques—SIGGRAPH '96, New Orleans, LA, USA, 4–9 August 1996; ACM Press: New York, NY, USA, 1996; pp. 31–42.
17. Levoy, M.; Zhang, Z.; Mcdowall, I. Recording and controlling the 4D light field in a microscope using microlens arrays. *J. Microsc.* **2009**, *235*, 144–162. [CrossRef] [PubMed]
18. Shogenji, R.; Kitamura, Y.; Yamada, K.; Miyatake, S.; Tanida, J. Bimodal fingerprint capturing system based on compound-eye imaging module. *Appl. Opt.* **2004**, *43*, 1355–1359. [CrossRef] [PubMed]
19. Dombrowski, M.; Catanzaro, B. Spatially Corrected Full-Cubed Hyperspectral Imager. U.S. Patent US7242478B1, 7 July 2007.

20. Shogenji, R.; Kitamura, Y.; Yamada, K.; Miyatake, S.; Tanida, J. Multispectral imaging using compact compound optics. *Opt. Express* **2004**, *12*, 1643. [CrossRef] [PubMed]
21. Hsieh, T.-C. MOS or CMOS Sensor with Micro-Lens Array. U.S. Patent US20060249765A1, 9 November 2006.
22. Moore, S. LSR claims advantages over clear thermoplastics in lighting applications. *Materials | Plastics Today*. Available online: https://www.plasticstoday.com/injection-molding/lsr-claims-advantages-over-clear-thermoplastics-lighting-applications/16893490760703 (accessed on 24 April 2020).
23. Sigloch, H. *Technische Fluidmechanik*, 6th ed.; Springer-Verlag: Berlin/Heidelberg, Germany, 2008.
24. Lu, D.; Wong, C.P. (Eds.) *Materials for Advanced Packaging*; Springer: New York, NY, USA, 2009.
25. Pecht, M.; Nguyen, L.T.; Hakim, E.B. (Eds.) *Plastic-Encapsulated Microelectronics: Materials, Processes, Quality, Reliability, and Applications*; Wiley: New York, NY, USA, 1995.
26. Hoster, B. Hochwertige Oberflächen für Duroplastische Formteile. In Proceedings of the 7th Internationale Duroplasttagung, Iserlohn, Germany, 17–18 April 2013.
27. Gardziella, A. *Duroplastische Harze, Formmassen und Werkstoffe: Chemie, Eigenschaften, Wirtschaftliche Bedeutung, Aktuelle Anwendungen und Technologien*; Expert Verlag: Renningen, Germany, 2000.
28. Schwarz, O. *Kunststoffkunde—Aufbau, Eigenschaften, Verarbeitung, Anwendungen, der Thermoplaste, Duroplaste und Elastomere*; Vogel-Verlag: Munchen, Germany, 2003.
29. Roeder, M.; Guenther, T.; Zimmermann, A. Review on Fabrication Technologies for Optical mold inserts. *Micromachines* **2019**, *4*, 233. [CrossRef] [PubMed]
30. Soltani, M.; Kulkarni, R.; Scheinost, T.; Groezinger, T.; Zimmermann, A. A Novel Approach for Reliability Investigation of LEDs on Molded Interconnect Devices Based on FE-Analysis Coupled to Injection Molding Simulation. *Multidiscip. Open Access J. IEEE* **2019**, *7*, 56163–56173. [CrossRef]